Mem. S.A.It. Vol. 79, 118

Memorie della

Models of comptonization

P.O. Petrucci

Laboratoire d'Astrophysique de Grenoble, UJF/CNRS, 414 rue de la Piscine, 38041 Grenoble Cedex 9, FRANCE
e-mail: pierre-olivier.petrucci@obs.ujf-grenoble.fr

Abstract. After a rapid introduction about the models of comptonization, we present some simulations that underlines the expected capabilities of Simbol-X to constrain the presence of this process in objects like AGNs or XRB

Key words. Radiation mechanisms: general

1. Introduction

The Compton effect was diskovered by A.H. Compton in 1923 and corresponds to the gain or loss of energy of a photon when it interacts with matter (usually electrons). For an electron at rest, the photon loss of energy is of the order

$$\Delta E = E' - E \simeq -\frac{E^2}{m_e c^2}(1 - \cos\theta)$$

where θ is the photon scattering angle (see Fig. 1).

For a on-stationnary electron part of the electron energy can be taken away by the photons (i.e. $\Delta E > 0$). This corresponds to the inverse Compton process.

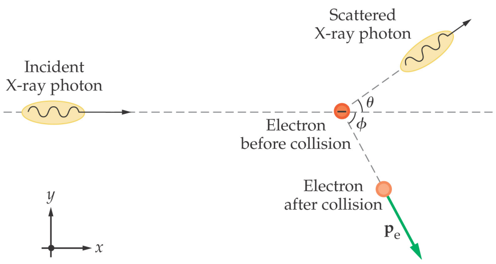

Fig. 1. A photon of energy E comes in from the left, collides with a target (usually an electron) at rest, and a new photon of energy E' emerges at an angle θ.

1.1. Thermal comptonization

Thermal comptonization corresponds to the case where seed photons (the "cold" phase) are comptonized by a thermal plasma (the "hot" phase) of electron. This thermal plasma is characterized by a temperature T_e and an optical depth τ. In this case, the mean relative energy gain per collision $\frac{\Delta E}{E}$ and the mean number of scatterings can be easily computed (e.g.

Send offprint requests to: P. O. Petrucci

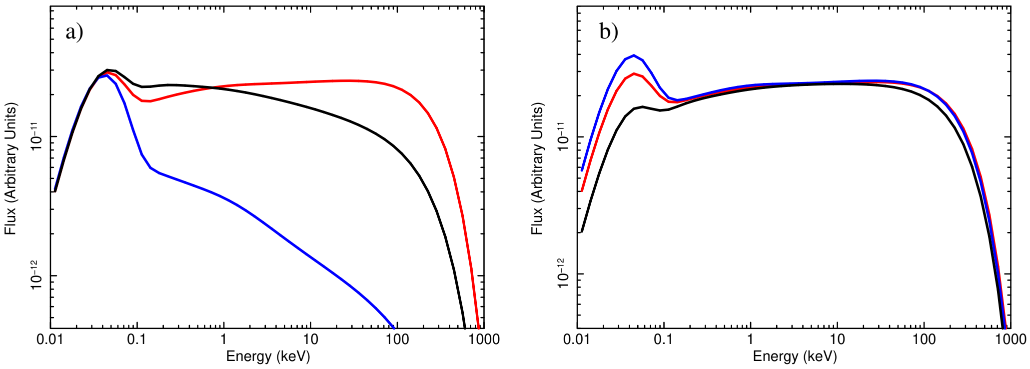

Fig. 2. a) Thermal comptonization spectra for the same plasma temperature and optical depth but different geometry: blue: cylindrical, red: slab, black: spherical. **b)** We fix the plasma temperature but change its optical depth in order to have roughly the same spectral index in the 2-10 keV band. This exemplifies the "geometrical" degeneracy of the thermal comptonization spectrum.

(Rybicki & Lightman, 1979)):

$$\frac{\Delta E}{E} \simeq \left(\frac{4kT_e}{m_e c^2}\right) + 16\left(\frac{kT_e}{m_e c^2}\right)^2 \text{ for } E \ll kT_e$$

and

$$N \simeq (\tau + \tau^2) \tag{1}$$

Then we define the Compton parameter $y = \frac{\Delta E}{E} N$. Large values of y means that the Comptonization process is efficient and modifies noticeably the seed spectrum.

1.1.1. Thermal comptonization spectrum

While thermal comptonization spectra have been computed since more than two decades, important effects like the anisotropy of the soft photon field were precisely taken into account in the beginning of the 90's by the pioneering works of Haardt (1993); Stern et al. (1995) and Poutanen & Svensson (1996). These effects appear far from being negligible. Noticeably, for a given set of plasma temperature and optical depth, the spectral shape is significantly different for different disk-corona geometries (cf. Fig. 2a) but also for different viewing angle, this last dependence being crucial for a correct interpretation of X-ray spectra. These effects underline the differences between realistic thermal comptonization spectra and the cut-off power law approximation generally used to mimic them. Moreover, the relation between the photon index Γ and the plasma temperature and optical depth can be strongly degenerated ("spectral" degeneracy) , different couples (τ, T_e) giving, for the same disk-corona geometry, the same Γ. A "geometrical" degeneracy also exists and is exemplified in Fig. 2b where the same high energy spectrum is reproduced with different set of parameters and with different geometries. These degeneracies complicate the fitting procedure and high S/N data over broad band energy intervals are required to break them.

1.1.2. Radiative balance

In a disk-corona system, the Comptonizing region and the source of soft photons are *coupled*, as the optically thick disk necessarily reprocesses and reemits part of the Comptonized flux as soft photons which are the seeds for Comptonization. The system must then satisfy equilibrium energy balance equations, which depend on *geometry* and on the ratio of direct heating of the disk to that of the corona.

In the limiting case of a "passive" disk (i.e. non intrinsically radiative, it radiates what it absorbs from the hot phase), the amplification of the Comptonization process, determined by the Compton parameter y, is fixed by geometry only (Haardt & Maraschi, 1991; Stern et al., 1995). Therefore, if the corona is in energy balance, the temperature and optical depth must satisfy a relation which can be computed for different geometries of the disk+corona configuration (cf. Fig. 3). It is then theoretically possible to constrain the geometry of the system and verify the selfconsistency of the model, provided that the plasma temperature and optical depth T_e and τ are known with sufficient precision.

1.2. Non-thermal comptonization

In the case of non-thermal particles the energy transfert between the elctron and the photon is very efficient. For an electron with a Lorentz factor γ it is of the order:

$$\Delta E \simeq \gamma^2 E \qquad (2)$$

Consequently the comptonization of a monoenergetic seed photon field by a non-thermal distribution of electrons $n(\gamma) \propto \gamma^{-s}$ produces a non-thermal spectrum $F(\nu) \propto \nu^{-\frac{s-1}{2}}$ (e.g. Rybicki & Lightman 1979).

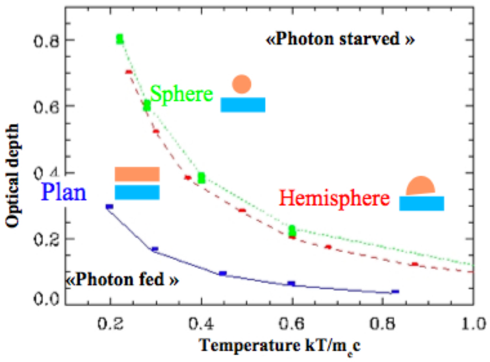

Fig. 3. Different theoretical relationship, corresponding to different disk-corona geometry, between the corona temperature and optical depth in the case of energy balance between the hot and cold phases.

2. What can we expect with SIMBOL-X?

The comptonization process play a role in all SIMBOL-X science cases,

– AGNs (thermal comptonization in Seyfert galaxies, non-thermal comptonization in Blazars)
– X-ray binaries (thermal comptonization in the hard state, non-thermal(?) comptonization in the Intermediate and Soft states)
– X-ray background
– Galaxy clusters
– Supernovae remnants
– GRBs

We detailed below some simulations of comptonization spectra showing the advances that we can expect with Simbol-X.

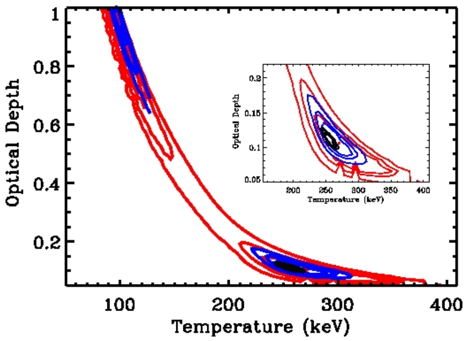

Fig. 4. Contour plots τ-kT_e for simulations of different exposures (red: 1ks, blue: 5 ks and black: 50 ks). The simulated data correspond to a thermal comptonization spectrum with $L_{2-10keV} = 10^{-11}$ erg.s−1.cm−2, $kT_e = 250$ keV, $\tau = 0$. Only the long exposure simulation enable to break the τ-kT_e degeneracy characteristic of thermal comptonization spectra.

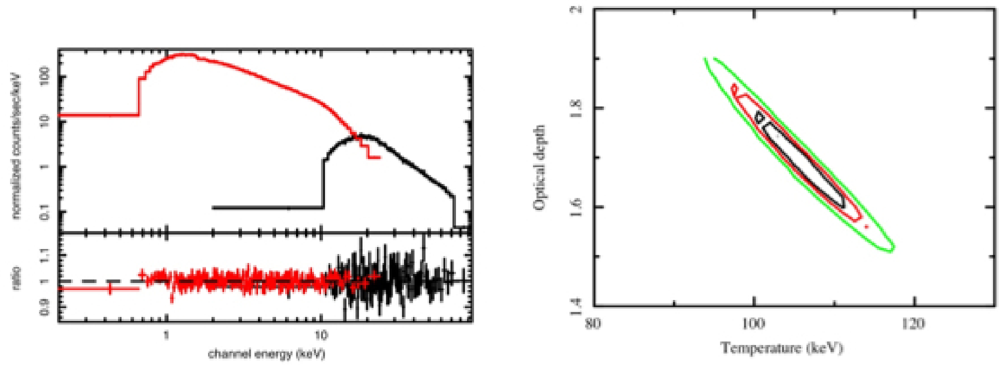

Fig. 5. Left: 500 sec. simulated Simbol-X data of Cyg X-1 assuming $L_{2-10keV} = 10^{-9}$ erg.s^{-1}.cm^{-2} $kT_e = 100$ keV, $\tau = 1.7$ and $R = 0.3$. Right: the corresponding τ-kT_e contour plot.

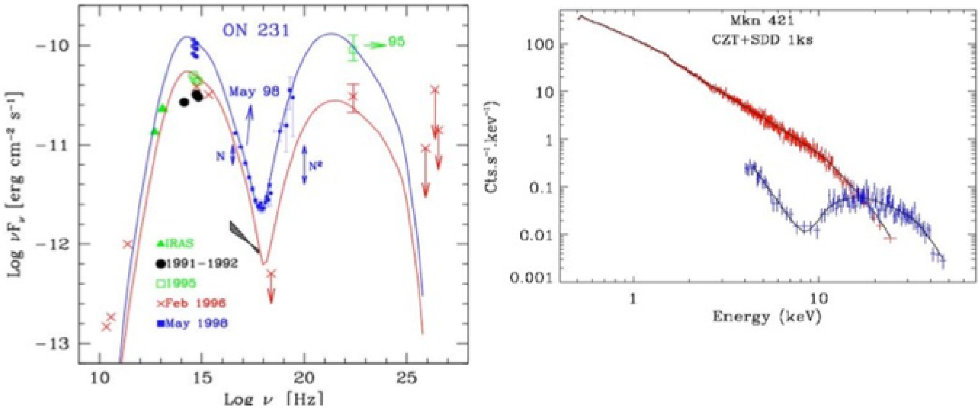

Fig. 6. Left: Typical Synchrotron Self-Compton spectrum of a blazar. Right: Simbol X simulation of the blazar Mkn 421 in 1ks.

2.1. Simu. N° 1: the case of a Seyfert galaxy

We simulate the spectrum of a Seyfert galaxy (NGC 5548) with different exposure time assuming $L_{2-10keV} = 10^{-11}$ erg.s−1.cm−2, kT_e = 250 keV, $\tau = 0.1$ and $R = 1$. We assume a slab geometry. Then we fit the faked data with the model used for the simulations. The corresponding contour plots τ-kT_e are plotted in Fig. 4. If, for small exposure time (1 ks, red contour plot) the contour is very elongated, this "spectral" degeneracy is broken for exposures of a few tens of ks (see the black contours that correspond to 50 ks). However we underline the fact that the real data generally show the presence of complex reflection/absorption features that can strongly limit the data analysis and the precise study of the underlying continuum.

It is worth noting that a few tens of ks corresponds to the orbiting timescale at a few Schwarzschild radii around a 10^8 solar masses black hole. It means that it should be possible with Simbol-X to follow the time evolution of the temperature and optical deth of the corona on a dynamical timescale. However simulations show that breaking the geometrical degeneracy will require very long (> 100 ks) exposure with Simbol-X.

2.2. Simu. N°2: the case of a microquasar

We simulate the X-ray spectrum of the microquasar Cyg X-1, with $L_{2-10keV} = 10^{-9}$ erg.s^{-1}.cm^{-2} $kT_e = 100$ keV, $\tau = 1.7$ and $R = 0.3$. Good constraints of the spectral parameters can be obtained in a few hundred of seconds (cf. Fig. 5).

2.3. Simu. N°3: the case of a blazar

We also simulate the X-ray spectrim of the blazar Mkn 421 (cf. Fig. 6). The spectrum is very well determine in 1 ks ! But in order to have constrains on the Synchrotron Self-Compton process multi-λ observations (radio, Optical, IR, X and γ) are needed.

3. Conclusions

- Simbol-X should bring strong constrains on comptonization spectra on dynamical time scale for AGNs, and on very short time scale in XrBs.
- However this can be complicated by the presence of complex absorption/emission features
- The broadest energy range is needed and multi-wavelength observations are recommended (CTA, GLAST, HERSCHEL, ALMA, LOWFAR, WSO-UV, ...).

Acknowledgements. I am grateful to the CEA/DSM/DAPNIA/SAp for its financial support.

References

Haardt, F. 1993, ApJ, 413, 680
Haardt, F. & Maraschi, L. 1991, ApJ, 380, L51
Poutanen, J. & Svensson, R. 1996, ApJ, 470, 249
Rybicki, G. B. & Lightman, A. P. 1979, in "A Wiley-Interscience Publication", New York: Wiley, 1979
Stern, B. E., et al. 1995, ApJ, 449, L13+